Civil Engineering
Engenharia Civil

RCC – Roller-Compacted Concrete with hematite aggregate

http://dx.doi.org/10.1590/0370-44672022760074

João Bosco Moreira Carmo[1,3]
https://orcid.org/0000-0002-3150-0281
Fernando Soares Lameiras[1,4]
https://orcid.org/0000-0002-3169-1647
Jose Marques Filho[2,5]
https://orcid.org/0000-0003-4404-274X
Walton Pacelli de Andrade[1,6]
https://orcid.org/0009-0003-6106-8818

[1]Centro de Desenvolvimento da Tecnologia Nuclear, Comissão Nacional de Energia Nuclear – CDTN/CNEN, Belo Horizonte - Minas Gerais - Brasil.

[2]Universidade Federal do Paraná - UFPR, Departamento de Construção Civil, Curitiba – Paraná - Brasil.

E-mails : [3]bosco.carmo@vale.com, [4]fsl@cdtn.br, [5]jmarquesfilho@gmail.com, [6]wpacelli@gmail.com

Abstract

RCC using hematite as an aggregate has interesting characteristics for use in massive structures or structures for radiation shielding. In Brazil, there is a considerable amount of hematite ore tailings without practical use, which makes this material an environmental problem and a matter of public safety. Thus, the search for alternatives to use these tailings is a priority environmental concern. An RCC containment dam with hematite aggregate was constructed to protect the basin of the Barao de Cocais River, including the city of Barao de Cocais in the State of Minas Gerais in Brazil, from a possible rupture of the Sul Superior tailings dam in the Congo Soco iron mine. Approximately 150,000 m^3 of RCC was deposited in three months. In this article, the results of the technological control tests during the construction of the containment are presented and compared with the results of the cores extracted after the construction, showing their coherence and strength performance compared with RCC using conventional aggregate. Also, studies related to the performance of radiation shielding of this RCC are presented. An attenuation of 10% of 1.6 MeV gamma radiation in relation to conventional concrete was observed.

Keywords: RCC, sustainability, recycled aggregate, hematite, radiation shielding.

1. Introduction

Roller-Compacted Concrete (RCC) is a concrete of no-slump consistency in its unhardened state that is typically transported, placed, and compacted using earth and rockfill construction equipment. If used in structures, special care should be taken to deal with heat generation from cementitious material hydration and the associated volume change that could generate thermal cracks. (Gencel, 2011). It allows a faster construction process compared with conventional concrete, with segregation control through the appropriate choice of the aggregate's granulometry.

In the Brazilian mix design approach, RCC has a high aggregate content and fine materials. It has less voids when compared to conventional concretes, using lower cement content, and therefore, presenting less retraction and cracking (Marques Filho, 2008; Gencel *et al*., 2010).

The history of RCC in dam works is presented in the ICOLD 2020 Bulletin (ICOLD, 2020) with recommendations in different countries and their experiences. Brazil has experience in RCC mixtures with high paste and low binder consumption, using aggregate fines of noble material passing in the 0.075 mm sieve and inhibiting expansive reactions (Campos, 2019).

An advantage of RCC is its lower cement content compared to conventional concrete, minimizing costs and greenhouse gas emissions. Since the compaction is made with large equipment, the obtained mass can withstand impact stresses due to their weight. The compressive strength required for massive structures, such as dams, is around 8 MPa at 90 days of control age. Moreover, due to the use of equipment, the amount of labor per unit volume is reduced when compared to conventional concrete, and the construction speed is significantly increased, generating a very efficient industrial process with measurable repetitive activities (Marques Filho, 2008).

Every year, millions of tons of tailings from iron ore mining are discarded in the region of the Iron Quadrangle in Minas Gerais, Brazil and stored in piles or dams. One of these tailings is the so-called GIC (Concentration Installation Granules). The GIC from the Água Limpa Mine has an iron oxide content below the attractive value but has a high absolute density, around 3.50 kN/m^3. It is an excellent option for RCC. Its high density provides a concrete density of 3.00 kN/m^3, allowing the construction of a massive structure with less volume and shorter execution time. It was successfully used in the construction of the containment dam in Gongo Soco, an iron mine operated by Vale in the municipality of Barao de Cocais – MG, Brazil. The purpose of this RCC dam was to contain the tailings from the Congo Soco dam that may be released in the event of its failure.

Hematite is normally used as an aggregate to obtain conventional heavy concrete for shielding from ionizing radiation (Gaber, 2016; Ouda & Abdelgader, 2019; Razali *et al*., 2019). High-density concrete can be used reliably and economically together with other protective materials to maximize protection from ionizing radiation (Vidhya & DhilipKumar, 2015). For example, heavy RCC using hematite tailings could be applied to regularize the foundation of a nuclear power plant, with the protection of aquifers and greater support capacity than foundations of compacted soils.

The objective of this article is to present the results of the technological control tests during the execution of the construction of the Gongo Soco RCC containment dam with hematite aggregate compared with the results of the probes extracted after the construction. Also, the results of the studies related to the radiation shielding of this RCC are also shown.

2. Material and method

The materials used to obtain the RCC were: 1) Portland cement with 50 wt% of ground granulated blast furnace (GGBF) slag; 2) GIC - Concentration Installation Granulates from the Água Limpa Mine; 3) Gneiss sand and gravel from the region with controlled fines to allow packing the grains together with cement paste; 4) Decanting water controlled according to the Brazilian Standard ABNT NBR 15900; 5) Air entrainer and retarding admixtures. The use of GIC was necessary to guarantee the construction schedule and to obtain high density. Initially, this material was sieved and classified between 50 mm and 12 mm size particles. Later it was used without any processing, since the loss due to sieving was about 50%, and this disposal would make it impossible to meet the pre-established schedule, without significant performance losses. Table 1 shows the characterization methods performed with these materials.

The RCC was produced continuously in a pug mill mixer and applied through the ramp-launching method that allows the continuous application of large volumes that are spread and compacted with road equipment. When application stoppages occurred, the horizontal joints were treated with surface waterblast cleaning and bonded with mortar applied before the next layer placement.

Due to the emergency need to build the dam in Congo Soco, the period to carry out the definition of the most suitable materials to compose the RCC and the mix design studies was short. In just over a month, samples of the materials were identified and sent to laboratories hired to provide technical support during the execution of the work (SOLOCAP in Belo Horizonte-MG and LACTEC in Curitiba-PR), which carried out the characterization and mix design studies.

The compressive strength tests of the RCC were performed according to the Brazilian standard method for cylindrical specimens with dimensions of 15 cm x 30 cm, molded on a vibrating table (ABNT, 2015a; ABNT, 2015b; ABNT, 2018a). The molding was performed in two layers with a vibration time of two minutes for each layer. The laboratory at Furnas Centrais Eletricas (in Goiania, Brazil) was hired to characterize the basic properties and carry out RCC special tests, with emphasis on the mechanical, elastic, visco-elastic, and thermal properties. In addition, the creep tests were performed in the same laboratory, measuring deformations with Carlson electrical extensometers embedded in the concrete. The stress control system was performed with RK MFL PRüfsysteme equipment and the compression-testing machine was the EMIC Brazil Model STB 120S. The tests were performed in a controlled environment (temperature of 23 ± 2°C and relative air humidity of 60 ± 10%). The applied loads were 35% of the rupture load obtained in the compressive strength tests. The direct shear strength tests were performed according to the ASTM D-5607/16 standard.

Table 1 – Characterization methods for the materials used to obtain the RCC.

Property	Methodology and/or equipment
Pozzolanic activity with lime and cement	ABNT NBR 5751:2015 /ABNT NBR 5752:2014
Portland cement – Brazilian requirements	ANBT NBR 16697:2018
Portland cement - Chemical analysis - determination of the main components by complexometry Part 2: ABNT test method	ABNT NBR NM 11-2:2012
Standard Specification for Portland Cement	ASTM C150/C150M-21
Ground aggregate Determination of expansion in mortar bars by the accelerated method	ABNT 15577-4:2018 Part 4
Petrographic analyzes of the GIC hematite tailings	Polished blades fragments. Qualitative mineralogical analysis was performed by X-ray diffraction (XRD) (D8 Advance X-ray Diffractometer from Bruker, total powder method, back loading)
Alkali-aggregate reaction	ABNT NBR 15577-3:2018

For the study of the actual hardened RCC, 70 m of cores with 1 m high and 15 cm diameter were extracted from the Gongo Soco containment dam through double-barrel rotary drilling with diamond bits, specific for the extraction of RCC cores, trying to minimize the extraction damages.

The core sampling campaign was programmed to prove the quality of the applied RCC and correlate it with the properties obtained during the construction. This campaign was performed by the company GEONORTE. The filming of the cores' extraction was carried out by the company GEOSOL. To verify the joint lifts mechanical parameters, untreated and treated joints with bonding mortar were tested in samples from the concrete cores by Solocap and PUC-RJ.

To perform the radiation shielding tests, three RCC blocks with the same composition as the one used to build the Gonco Soco containment dam and three conventional concrete blocks using common aggregates in both cases with cubic format of 15 cm edge were cast and molded by Solocap. The conventional concrete blocks used the RCC mix design proportions, but with gneiss aggregates from nearby the Gongo Soco Mine. This concrete has a compressive strength very close to the RCC results and lower permeability. The molding of these blocks was carried out in the laboratory on a vibrating table to achieve characteristics similar to the concrete applied at the dam.

The blocks were irradiated in a Multipurpose Panoramic Irradiator of Category II, manufactured by MDS Nordion, model/series IR-214 and GB-127 type, equipped with a cobalt-60 source with a nominal absorbed dose of 100 Gy at 50 cm from the source. To evaluate the shielding, a 20 cm x 20 cm radiochromic film was positioned on the posterior face of the blocks. A second block was positioned behind the radiochromic film to minimize the influence of the scattered radiation in the irradiation chamber. Gafchromics EBT radiochromic films from the International Speciality Products (ISP) were used. To quantify the distribution of absorbed doses recorded by each film, a sensitometry test was performed, in which samples of the same film were radiated with different absorbed doses to correlate the darkening degree of the film to the corresponding absorbed dose. Dose is the energy absorbed from the gamma rays per unit mass, measured in Grays, 1 Gray (Gy) = 1 J/kg. These tests were performed without the block in front of the film. The films were scanned in a HP Scanjet 4050 scanner with 300 DPI resolution. Digitized images were converted into numerical data containing the coordinates (x, y, z), where x and y correspond to the Cartesian coordinates of the film's plan and z corresponds to the color intensity of the green channel of the RGB image. From the data, 3D and 2D images were generated to describe the distribution of doses on the surface of the film, and consequently, the shielding of the block.

3. Results

The results of mineralogical characterization of the GIG are shown in Table 2. Figure 1 shows images of the microstructure of the GIC.

Table 2 – Mineralogical characterization of the GIC – Concentration Installation Granulate from Agua Limpa Mine.

Minerals	wt%	Chemical compositiona	wt%
Magnetite	0.50	Fe_{total}	39.75
Microcystalline Hematite	0.49	Fe_2O_3	57.47
Hematite in Martite	0.77	FeO	0.32
Granular Hematite	12.13	SiO_2	38.35
Lamellar Hematite	40.46	Al_2O_3	0.45
Earth Goethite	1.85	MgO	1.04
Quartz	37.18	Na_2O and F	0.02
Amphibole	1.18	CaO	1.23
Carbonate	3.59	K_2O	0.30
Others	1.85	H_2O	0.30
Total	100.00	CO_2	1.71

[a] Approximated and based on the theoretical composition of minerals.

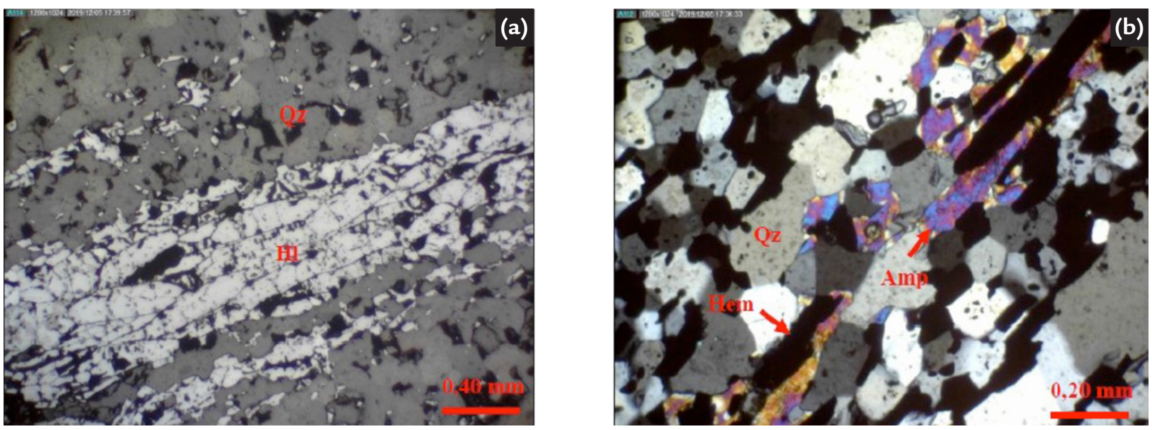

Figure 1 – Mineralogy and photomicrography of a fragment from the GIC – Concentration Installation Granulate from Agua Limpa Mine. a) Weft aspect, banding detail with levels sometimes richer in quartz (Qz), sometimes in lamellar hematite (Hl). Reflected light, parallel nichols, 2.5x objective and 10x eyepieces. b) Weft aspect Quartz (Qz) and amphibolite (Amp) granoblasts associated with hematite (Hem) crystals. Transmitted light, crossed nichols, 5x objective, 10x eyepieces.

The hematite tailings (GIC) generated at the Agua Limpa Mine was transported to the Congo Soco mine by rail. The other aggregates of gneiss origin were supplied by quarries in the region and were also transported by rail, which streamlined the logistics of supplying aggregates for the study.

The RCC mix was chosen based on the cubic curve proposed by Bolomey (Andriolo, 1998) admitting a ±5% range. The granulometric curve of the mixture was close to the theoretical curves, as can be seen in Table 3 and Figure 2. The original gneiss gravel with maximum dimension of 25 mm was introduced in the mixture to improve the fit of the theoretical curve of granulometry. Table 4 shows the results of X-ray analysis on RCC.

Table 5 shows the results of the RCC in the preliminary studies and during construction.

Table 3 – Granulometry of the aggregate components and composition used in the CCR, compared with the Bolomey curves (Andriolo, 1998).

Sieve (mm)	Components			CCR composition	Bolomey curves		
	Artificial sand mixture	Gravel	GIC 50-0				
	40%	10%	50%		Bottom	Average	Top
	Retained accumulated (%)						
50	0.00	0.00	0.00	0.00	0.00	0.00	5.00
38	0.00	0.0	8.10	4.05	3.74	8.74	13.74
25	0.00	3.4	26.95	13.82	15.63	20.63	25.63
19	0.00	11.1	35.31	18.77	22.57	27.57	32.57
9.5	0.00	89.0	58.95	38.38	37.51	42.51	47.51
4.8	5.63	98.0	73.73	48.92	49.21	54.21	59.21
2.4	22.7	98.3	77.16	57.49	58.66	63.66	68.66
1.2	35.25	98.3	78.67	63.27	66.16	71.16	76.16
0.6	46.75	98.3	80.05	68.56	72.11	77.11	82.11
0.3	58.79	98.3	82.09	74.39	76.83	81.83	86.83
0.15	80.62	98.3	89.06	86.61	80.58	85.58	90.58
0.75	86.79	100.0	96.78	93.11	83.55	88.55	93.55
Fineness modulus	2.50	6.90	5.83	4.60	4.67	5.12	5.57

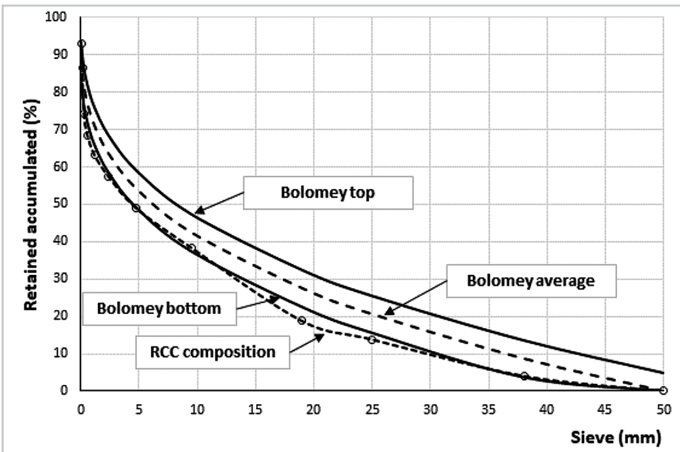

Figure 2 – Granulometry of the RCC aggregate composition compared with the Bolomey curves.

Table 4 – X-ray analyses on the ground RCC.

X-ray diffraction			
JCPDF/ICDDa	**Compound name**	**Chemical formula**	**wt%**
00-005-0490	Quartz	SiO_2	35.63
00-024-0072	Hematite	Fe_2O_3	37.90
00-018-1202	Anorthite	$Na_xCa_{1-x}Al_{2-x}Si_2+_xO_8$	2.92
00-023-1405	Edenite	$NaCa_2Mg_5Si_7AlO_{22}(OH)_2$	3.66
00-019-0932	Microcline	$KAlSi_3O_8$	7.57
00-007-0078	Clinochlore	$(Mg,Fe^{++})_3Al(Si_3Al)O_{10}(OH)_8$	2.16
00-042-1437	Biotite	$K(Mg,Fe^{++})_3(AlSi_3O_{10})(F,OH)_2$	6.75
00-024-0027	Calcite	$CaCO_3$	1.88
00-036-0426	Dolomite	$CaMg(CO_3)_2$	0.98
00-013-0558	Talc	$Mg_3Si_4O_{10}(OH)_2$	0.55

X-ray fluorescence												
Loss on ignition	**Al_2O_3**	**CaO**	**Cr_2O_3**	**Fe_2O_3**	**K_2O**	**MgO**	**MnO**	**Na_2O**	**P_2O_5**	**SiO_2**	**TiO_2**	**SO_3**
2.54	4.14	2.59	0.00	43.71	1.13	0.69	0.11	0.25	0.02	44.33	0.14	0.14

[a] JCPDF software with the standard charts from the ICDD - The International Centre for Diffraction Data.

Table 5 – Results of the preliminary studies and during construction.

Service Front Laboratory			Preliminary Studies in Lab	Quality Control During Construction	
	Date		05/07/2019	Sep - Dec 2019	
	Cement (kN/m³)		0.99	1.00	
	Water (kN/m³)		1.43	1.40	
	Artificial sand (kN/m³)		9.44	10.87	
	GIC (kN/m³)		17.53	14.49	
	Air entrainer admixture (%)		1.0	1.6	
	Retarding admixture (%)		0.99	1.00	
	Water/Cement		1.44	1.40	
	Specific gravity (kN/m³)		29.40	29.85	
	Room temperature (°C)		23	-	
RCC Fresh Properties	Cannon Time (s)		9	12	
	Specific Gravity Vebe (kN/m³)		29.59	29.61	
	Entrained Air (%)		1.0	1.6	
	Temperature (° C)		23	21	
Number of samples			2	224	
Hardened RCC (MPa) Compressive Strength	7 days	3.2	3.1	Mean	3.4
		Mean = 3.15	Standard deviation = 0.071	Standard deviation	1.2
		95% confidence interval: 2.51 – 3.79		95% confidence interval: 3.24 – 3.56	
	28 days	6.8	6.9	Mean	6.6
		Mean = 6.85	Standard deviation = 0.071	Standard deviation	1.9
		95% confidence interval: 6.21 – 7.49		95% confidence interval: 6.35 – 6.85	
	90 days	9.7	9.2	Mean	10.5
		Mean = 9.45	Sandard deviation = 0.354	Standard deviation	2.1
		95% confidence interval: 6.27 – 12.63		95% conficende interval: 10.22 – 10.78	

The results of the special tests carried out by Furnas Laboratory is shown in Table 6. Figure 3 shows the adiabatic temperature rise of the RCC. All alkali-aggregate reactivity tests performed showed innocuous results with cement alkalis. Table 7 shows the results of the regression curve shown in equation (1) to the creep data of RCC samples. Figure 4 shows the fit of equation (1) for one of the samples of RCC with 28 days of curing.

$$\varepsilon_{elastic\ +\ specific} = f(k)\ .\ \ln\ (t+1) + \frac{1}{E} \qquad (1)$$

where ε is the deformation, $f(k)$ is the creep coefficient and E is the elastic modulus.

Creep results are comparable with traditional creep curves obtained for concrete (Andriolo, 1998).

Table 6 – Characterization of the RCC – Furnas Laboratory – Goiânia - Goiás - Brazil.

Property at 28 Days of Age	Result
Flexural strength by diametral compression (MPa)	1.5
Compressive strength (MPa)	10.5
Elasticity module (GPa)	14.6
Adiabatic temperature rise (°C)	5.5
Thermal expansion coefficient (x10^{-6} /°C)	9.5
Thermal diffusivity at 40 oC (m²/day)	0.1022
Thermal conductivity (J/m.s.K)	3.53
Specific heat (saturated) (J/kg.K)	995
Permeability coefficient (10^{-11} m/s)	7.23

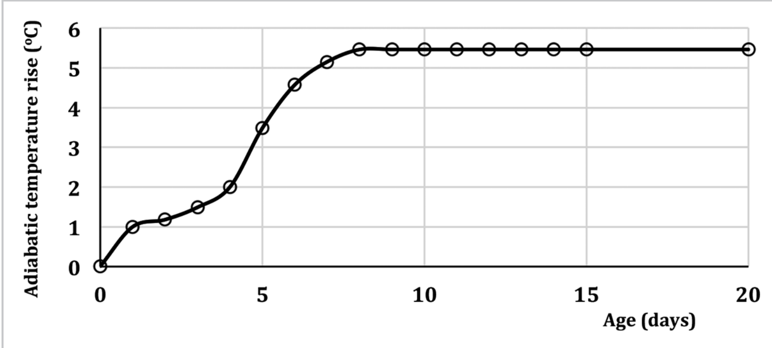

Figure 3 – RCC adiabatic temperature rise (cement with 50% granulated blast furnace slag).

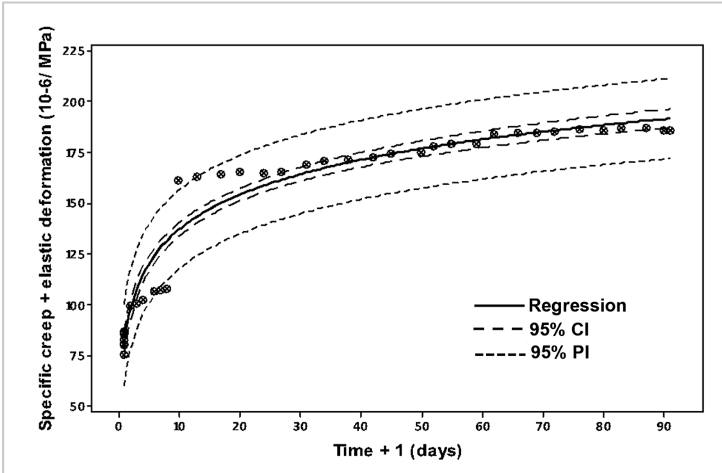

Figure 4 – Regression curve presented by Equation (1) for sample 2 representing 28 days of curing (with 95% confidence and prediction intervals).

Table 7 – Fit of equation (1) to the creep measurements on CCR samples.

Curing →	5 days		7 days		28 days	
Samples →	1	2	1	2	1	2
f(k) (10^{-6}/MPa)	15.40	28.90	32.73	25.63	23.92	24.87
1/E (10^{-6}/MPa)	580.82	683.69	169.47	179.34	68.65	79.66
R^2 (%)	64.47	91.03	89.34	76.81	93.85	94.84
E (GPa)	1.72	1.46	5.90	5.58	14.57	12.55

The results of the tests performed on the cores extracted from the RCC containment dam are shown in Table 8. The cores proved that the combination of aggregates and the water content of the RCC resulted in good interlocking.

Table 8 – Results of the tests performed in the cores extracted from the RCC containment dam.

Borehole code	SRC-01	SRC-02A	SRC-05	SRC-06	SRC-07
Density (kN/m³)	30.94	31.48	29.53	29.24	30.43
Water absorption (%)	5.2	4.8	5.3	5.8	4.2
Compressive strength (MPa)	11.9	11.4	10.9	10.7	11.5
Tension strength - Brazilian Test (MPa)	1.6	1.4	1.4	1.6	1.4
Elasticity Modulus (GPa)	13.1	14.3	19.6	14.2	8.0
Permeability Coefficient (10^{-11} m/s)	6.82	9.79	8.35	9.13	7.39
Direct shear					
Type of joint	Treated		Untreated		
Laboratory	Solocap	PUC-RJ	Solocap		
Cohesion (MPa)	0.899	0.690	0.614		
Friction angle (Degrees)	45.1	48.4	70.1		

Table 9 shows the average absorbed dose measured on the radiochromic films positioned behind for RCC and conventional concrete samples. A dose reduction of 10% was observed for RCC. Figure 5 shows the dose distribution observed on the radiochromic films.

Table 9 – Theoretical thicknesses of concretes required for shielding.

Concrete	Average specific mass (kN/m^3)	Average absorbed dosis (Gy)	Absorbed dose reduction (%)
RCC with GIC	29.05	15.696	10
Conventional concrete	23.06	23.977	

Figure 5 also shows that the shielding of gamma radiation was not uniform across both blocks. This was probably due to the segregation of the aggregates, but the shielding of the RCC block was more uniform, perhaps due to the lower segregation. The RCC shielding was 10% higher than conventional concrete.

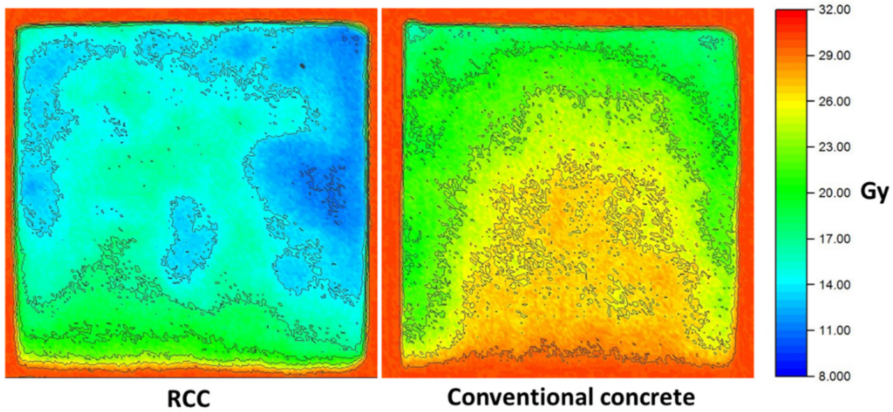

Figure 5 – Qualitative comparison of the shielding of gamma radiation of samples of RCC (left) and conventional concrete (right). The blue color means the lower dose measured at the radiochromic film (higher shielding) and the red color the higher dose (lower shielding).

The results demonstrate that it is adequate to use RCC in gravity dam construction, since it attended all the design required criteria and parameters. The construction has been significantly fast and efficient, with an average concrete placement and compaction of 70,000 m^3/month, and no problems have been detected due to the use of hematite tailings aggregate.

RCC laboratory samples with hematite aggregate showed a shielding of gamma irradiation 10% greater than conventional concrete samples.

The results obtained by the RCC applied in Gongo Soco met the parameters specified by the WALM Designer. The values obtained with the RCC are considered compatible in similar structures and the use of hematite tailings proved to be a suitable material that can be applied in other works with similar purposes. The RCC using these tailings aggregates can be applied in dam construction, and it demonstrated its efficiency in the emergency works necessary to create a contention dam to minimize risks due a possible tailings dam stability problem. The study results indicate the technical feasibility of the use of the iron waste tailings as recycled aggregate in massive concrete structures. In addition. the radiation studies indicate that the material could be considered for containment and shielding works in radiological accidents, or for foundations of nuclear plants.

4. Conclusions

A RCC containment dam with hematite aggregate was constructed to protect the basin of the Barao de Cocais River in the State of Minas Gerais in Brazil from a possible rupture of the Sul Superior tailings dam in the Congo Soco iron mine. Cores extracted from this containment showed a density of 29.85 kN/m^3, compressive strength of 10.5 MPa, and water absorption of 5%, according to the design.

The use of Portland cement with 50% of blast furnace slag promoted an adiabatic temperature increase of 5.5°C, observed in laboratory samples, suitable for the use of this RCC in massive structures. Laboratory samples with 28 days of curing showed total strain (elastic strain plus specific creep) of 175.10^{-6}/MPa at 90 days of creep testing. The modulus of elasticity ranged from 12.0 to 14.6 GPa. The cores extracted from the containment dam showed elastic moduli between 8 and 19 GPa, a diametrical compressive strength of 1.4 to 1.6 MPa, and a permeability coefficient between 6.10^{-11} and 10.10^{-11} m/s. In the direct shear test, the joints treated with mortar showed cohesion between 0.7 and 0.9 MPa and friction angles between 40° and 48°. Untreated joints showed a cohesion of 0.6 MPa and a friction angle of 70°.

Acknowledgments

The authors are thankful for the support of Vale S. A. and CDTN, as well as the CMM Consortium and INCT Midas.

References

ANDRIOLO, F. R. ***The use of the roller compacted concrete.*** São Paulo: Oficina de Textos, 1998. 584 p.

ASSOCIAÇÃO BRASILEIRA DE NORMAS TÉCNICAS - ABNT. ***NBR 16312-2***: roller compacted concrete – part 2: preparation in laboratory = concreto compactado com rolo – parte 2: preparação em laboratório. Rio de Janeiro, 2015a.

______. ***NBR 16312-3***: roller compacted concrete – part 3: laboratorial tests in fresh concrete = concreto compactado com rolo – parte 3: ensaios de laboratório em concreto fresco. Rio de Janeiro, 2015b.

______.. ***NBR 5739: concrete*** – compression test of cylindrical specimens = concreto – ensaio de compressão de corpos de prova cilíndricos. Rio de Janeiro, 2018.

AMERICAN SOCIETY FOR TESTING AND MATERIALS. ***ASTM D-5607/16***: standard method for performing laboratory direct shear strength tests of rocks specimens under constant normal force. Philadelphia, 2016.

CAMPOS, H. F. ***Dosage of sustainable and high strength concrete optimized by particle packaging models with partial replacement of Portland cement by stone powder and active silica.*** Tese (Doutorado). Universidade Federal do Paraná, Curitiba, 2019.

CARMO, J. B. M. The use of concrete-rock contact cohesion parameter in the sizing of the containment wall at Gongo Soco Mine (RCC Dam). *In*: DAM WORLD CONFERENCE, 4, 2020. Lisboa: LNEC, 2020. v. 1.

COMISSÃO NACIONAL DE ENERGIA NUCLEAR. ***CNEN NN 3.01***: basic radiological protection = diretrizes básicas de proteção radiológica. Rio de Janeiro, 2014.

GABER, M. A. W. Assessment of Bahariya hematite-barite ore as a heavy weight concrete mix for subsea pipeline cladding. ***Research Journal of Applied Sciences***, v. 12, n. 9, p. 955-963, 2016.

GENCEL, O. Physical and mechanical properties of concrete containing hematite as aggregates. Science and Engineering of Composite Materials, v. 18, p. 191-199, 2011.

GENCEL, O. *et al*. Concretes containing hematite for use as shielding barriers. ***Materials Science***, v. 16, n. 3, p. 249-256, 2010.

GURLER. O.; TARIM. U. A. An investigation on determination of attenuation coefficients for gamma-rays by Monte Carlo method. ***Journal of Radioanalytical and Nuclear Chemistry,*** v. 293, p. 397-401, 2012.

INTERNATIONAL COMMISSION ON LARGE DAMS. ***Roller compacted concrete dams. London***: CIGB ICOLD, 2020. 426 p. Bulletin 177.

MARQUES FILHO, J. *et al*. Development of laboratory device to simulate roller-compacted concrete placement. ***ACI Materials Journal,*** v. 105, p. 125-130, 2008.

OUDA, A. S.; ABDELGADER, H. S. Assessing the physical mechanical properties and γ-ray attenuation of heavy density concrete for radiation shielding purposes. ***Geosystem Engineering,*** v. 22, n. 2, p. 72-80, 2019.

RAZALI, M. E.; HAMID, R.; ABDULLAH, Y. Mechanical properties and thermal neutron absorption of Heavyweight hematite aggregate concrete for radiation shielding. ***International Journal of Engineering & Technology,*** v. 8, n. 1.2, p. 123-130, 2019.

VIDHYA, K.; DHILIPKUMAR, R. An experimental investigation on strength characteristic of High-Density concrete incorporating hematite. ***IJIRST – International Journal for Innovative Research in Science & Technology,*** v. 2, n. 7, p. 61-66, 2015.

Received: 22 November 2022 - Accepted: 5 April 2023.